Remote Sens. **2010**, *2*, 1496-1507; doi:10.3390/rs2061496

OPEN ACCESS

Remote Sensing

ISSN 2072-4292

www.mdpi.com/journal/remotesensing

Article

Medium Spatial Resolution Satellite Imagery to Estimate Gross Primary Production in an Urban Area

A. Rahman As-syakur [1,2,*], Takahiro Osawa [2] and I. Wayan S. Adnyana [1, 2]

[1] Environmental Research Center, Udayana University, PB Sudirman Street, Denpasar, Bali 80232, Indonesia; E-Mail: sandiadnyana@yahoo.com

[2] Center for Remote Sensing and Ocean Science (CReSOS), Udayana University. PB Sudirman Street, Post Graduate Building, Denpasar, Bali 80232, Indonesia; E-Mail: osawa320@gmail.com

* Author to whom correspondence should be addressed; E-Mail: ar.assyakur@pplh.unud.ac.id; Tel.: +62-361-236-221; Fax: +62-361-236-180.

Received: 6 April 2010; in revised form: 10 May 2010 / Accepted: 21 May 2010 / Published: 3 June 2010

Abstract: Remote sensing data with medium spatial resolution can provide useful information about Gross Primary Production (GPP), especially on the scale of urban areas. Most models of ecosystem carbon exchange that are based on remote sensing use some form of the light use efficiency (LUE) model. The aim of this work is to analyze the distribution of annual GPP in the urban area of Denpasar, Bali. Additional analysis using two types of satellite data (ALOS/AVNIR-2 and Aster) addresses the impact of spatial resolution on the detection of various ecosystem processes in Denpasar. Annual GPP estimated using ALOS/AVNIR-2 varied from 0.13 gC m^{-2} yr^{-1} to 2,586.18 gC m^{-2} yr^{-1}. Meanwhile, the Aster estimate varied from 0.14 gC m^{-2} yr^{-1} to 2,595.26 gC m^{-2} yr^{-1}. GPP as measured by ALOS/AVNIR-2 was lower than that from Aster because ALOS/AVNIR-2 has medium spatial resolution and a smaller spectral range than Aster. Variations in land use may influence the measured value of GPP via differences in vegetation type, distribution, and photosynthetic pathway type. The medium spatial resolution of the remote sensing data is crucial for discriminating different land cover types in heterogeneous urban areas. Given the heterogeneity of land cover over Denpasar, ALOS/AVNIR-2 detects a smaller maximum value of GPP than Aster, but the annual mean GPP from ALOS/AVNIR-2 is higher than that from Aster. Based on comparisons with previous work, we find that ALOS/AVNIR-2 and Aster satellite data provided more accurate estimates of maximum GPP in Denpasar and in the tropical Kalimantan-Indonesia and Amazon forest than estimates derived from the MODIS GPP product (MOD17).

Keywords: ALOS/AVNIR-2; Aster; gross primary production; spatial resolution

1. Introduction

The most important global interactions between the biosphere and atmosphere involve the transfer of energy, water, and carbon. Carbon is assimilated by the biosphere through photosynthesis and released through autotrophic and heterotrophic respiration [1]. Emissions and re-absorption of carbon gases from natural ecosystems were in a state of equilibrium for millions of years; however, this balance has been disturbed by human activities. Consequently, atmospheric concentrations of carbon dioxide (CO_2) have been increasing and are widely believed to be responsible for global warming [2]. Understanding the drivers of the spatial and temporal patterns of surface-atmosphere CO_2 exchange is therefore crucial to improving predictions of future concentrations of atmospheric CO_2 [3]. To achieve this goal, plant cover and corresponding surface CO_2 uptake must be monitored on a large scale. Such data will facilitate accurate estimates of regional and global carbon budgets and, ultimately, more accurate prediction of carbon source-sink relationships and atmospheric CO_2 concentrations [4]. Remote sensing can be used to estimate surface-atmosphere CO_2 exchange such as gross primary productivity (GPP).

GPP is the total carbon assimilated by vegetation [5]. Based on biological processes GPP is the sum of net primary productivity (NPP) with respiration. GPP can be estimated by combining remote sensing with carbon cycle processing [6]. GPP have been estimated based on biophysical parameters derived from vegetation indices (such as the normalized difference vegetation index, NDVI), land-cover data, and light-use-efficiency parameters [7]. Most models of ecosystem carbon exchange that are based on remote sensing use some form of the light use efficiency (LUE) model. The LUE model states that carbon exchange is a function of the amount of light energy absorbed by vegetation and the efficiency with which that light energy is used to fix carbon [8]. Monteith [9] developed a method for estimating plant productivity from observations of APAR and estimates of LUE.

Remotely-sensed optical signatures have proved useful for estimating a range of ecological variables including leaf area index (LAI) and the absorptivity of photosynthetically active radiation (APAR) [10,11]. The fraction of absorbed photosynthetically active radiation (fAPAR) driven by vegetation cover is related to the NDVI. The strong relationship between NDVI and fAPAR has been examined in detail through theoretical and experimental analyses [10,12,13]. The NDVI has become a popular tool for assessing different aspects of plant processes while simultaneously determining spatial variation in vegetation cover [14].

Previous work in the Kalimantan tropical forest estimated a GPP value of between 2,859 and 3,227 gC m^{-2} yr^{-1} [15], and research in an Amazonian tropical forest showed a GPP of 3,040 gC m^{-2} yr^{-1} [1]. The seasonal dynamics of GPP prediction from satellite data were similar to those of GPP from observations. Seasonally-integrated GPP observations over an eight-month period accounted for 98% of the annual GPP prediction [16]. In a tropical evergreen forest in the Brazilian Amazon, prediction of GPP from MODIS satellite data was consistent with GPP estimation from eddy flux tower measurements [17,18], with a GPP prediction from MODIS of about 2,977 gC m^{-2} $year^{-1}$ [17]. Research in the Labanan Concession Area in the East Kalimantan area of Indonesia showed an annual range of GPP from 1,710 to 2,635 gC m^{-2} $year^{-1}$ based on MODIS satellite data [19]. Estimates of

GPP from Landsat were linearly related to daytime maize GPP measurements with root mean squared error less than 1.58 gC m^{-2} d^{-1} over a GPP range of 1.88 to 23.1 gC m^{-2} d^{-1} [20].

Denpasar represent an urban city in Bali. Remote sensing is a tool for mapping and monitoring urban areas. Application of remote sensing data for urban areas requires imagery with moderate until high spatial resolution. Remote sensing is a powerful tool for mapping and monitoring regional landscapes, and high-resolution imagery has proved effective for understanding land properties (e.g., ecosystems and hydrology) [21] and vegetative cover [22] in urban areas. Landsat imagery with a moderate spatial resolution of 30 m has been effectively used to classify homogeneous landscapes; however, the accuracy of such techniques may diminish in regions with highly heterogeneous landscapes [22]. Urban areas provide unique challenges to satellite remote sensing techniques. In urban landscapes, accurate flux measurements are complicated by surface heterogeneity, and NDVI is less useful for estimating CO_2 exchange [23]. The operational potential of urban remote sensing depends on the capacity of remote sensing to capture small-scale objects over heterogeneous surfaces in urban areas [24]. We therefore require imagery with spatial resolution higher than that of Landsat to classify and identify the heterogeneous landscapes characteristic of urban areas. ALOS/AVNIR-2 and Aster are two types of images that have higher spatial resolution than that of Landsat. ALOS/AVNIR-2 has a spatial resolution of 10 m and Aster 15 m in the red and near infrared (NIR) bands. The spatial resolution of the remote sensing data is crucial for discriminating fluxes for the different land cover types and hence avoiding significant errors due to application of a land surface model to a mixed pixel containing large contrasts in vegetation cover [25].

The aim of this research is to analyze the potential of GIS and remote sensing for estimating GPP, in particular over urban scales. In this study, we focus our analysis on the distribution of annual GPP, which effectively measures CO_2 assimilation by vegetation in urban areas. We further use two types of satellite data (ALOS/AVNIR-2 and Aster) to assess the impact of spatial resolution on the detection various ecosystem processes in Denpasar, an urban city in Bali Island, Indonesia.

2. Research Methods

2.1. Research Location and Materials

The research was conducted in Denpasar, a city in the Province of Bali, Indonesia, located at 8°36′56″S–8°42′01″S and 115°10′23″E–115°16′27″E (Figure 1) The location is between two neighborhood regencies namely Badung and Gianyar Regencies. Denpasar city population reached 608,595 people in 2007. The condition of oblique topography is from north to south with the height level of 0–75 m above sea level, while the inclination slope morphology is from 0 to 5%. Denpasar has tropical climate with monthly mean temperature around 24–32 °C and monthly mean precipitation around 13–358 mm. The dominant land use in Denpasar is the settlement that has an area of 7,179.17 ha.

Figure 1. The research location: Denpasar, Bali, Indonesia.

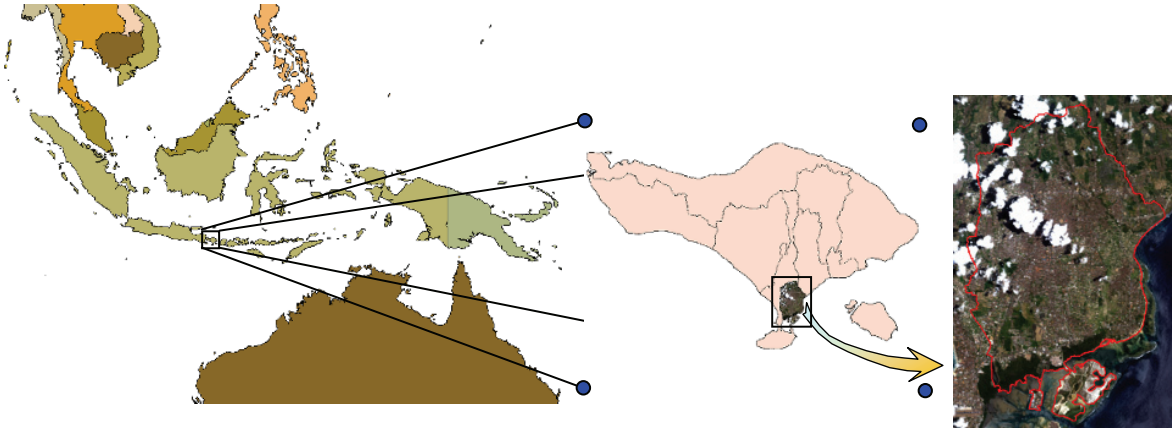

The following materials were used in this work: (1) a digital image of the Denpasar area taken on 13 October 2006 from ALOS/AVNIR-2, (2) a digital image of the Denpasar area taken on 5 September 2006 from Aster, (3) a land use map of the Denpasar area in 2006 from Quick Bird, (4) a topography map of the Denpasar region at a scale of 1:25,000 from the Indonesian National Coordinating Agency for Surveys and Mapping (Bakosurtanal), and (5) solar radiation data from the Indonesian Meteorology, Climatology and Geophysics Agency (BMKG). ALOS/AVNIR-2 and Aster images were used to calculate the value of GPP. Topographic maps were used for coordinate corrections. Meanwhile, solar radiation data was used to calculate photosynthetically active radiation (PAR).

2.2. Radiance Correction

Digital numbers (DN) in each band of the ALOS/AVNIR-2 and Aster images were converted to physical measurements of sensor radiance (L_{sat}). Conversion of DN to absolute radiance values is a necessary procedure for comparative analysis of several images taken by different sensors [26]. Since each sensor has its own calibration parameters used in recording the DN values, the same DN values in two images taken by two different sensors may represent two different radiance values. For this purpose we used the following formula, which implicitly includes a transformation of the analog signal received at the sensor to DN stored in the resulting image pixels (Equation 1):

$$L_{sat} = (DN + a) \times UCC \quad (1)$$

Here, a represents the absolute calibration coefficients contained in the header file (0 for ALOS/AVNIR-2 [27] and −1 for Aster satellite data [28]), and UCC is the Unit Conversion Coefficient, which is different for each image band and also depends on the gain setting that was used to acquire the image. Values of UCC for ALOS/AVNIR-2 and Aster images are given in Table 1.

Table 1. Unit Conversion Coefficient (UCC) for each band of satellite imagery.

ALOS/AVNIR-2		Aster	
Band No	UCC	Band No	UCC
1	0.588	1	0.676
2	0.573	2	0.708
3	0.502	3N	0.862
4	0.835		

2.3. Data Analysis

The carbon budget is controlled by several major processes that describe the exchange of carbon dioxide between terrestrial ecosystems and the atmosphere. Satellite remote sensing provides consistent and systematic observations of vegetation and has played an increasingly important role in characterizing vegetation structure and in estimating the GPP of vegetation [16]. In this work, GPP was estimated using the following equation:

$$GPP = \varepsilon \times fAPAR \times PAR = \varepsilon \times APAR \quad (2)$$

PAR is restricted to the visible portion of the solar spectrum, *i.e.*, from 400 to 700 nanometers [29]. PAR is assumed to be approximately half of the incoming solar radiation [30], with solar radiation data from the Indonesian Meteorology, Climatology and Geophysics Agency (BMKG). The fAPAR is related to the NDVI. NDVI has been widely used to estimate fAPAR because of the positive linear relationship between these variables [12]. In Southeast Asian countries, this relationship can be parameterized as [31]:

$$fAPAR = -0.08 + 1.075 \times NDVI \quad (3)$$

NDVI is computed from image data using the following formula:

$$NDVI = \frac{\text{Near Infra Red Band - Red Band}}{\text{Near Infra Red Band + Red Band}} \quad (4)$$

Light use efficiency (ε) is a biome-specific value representing the optimal potential of the vegetation to convert PAR to GPP. Light use efficiency values are similar for all plant types and biomes [29]. Estimation of LUE has proven problematic since it varies with vegetation type and environmental conditions. Light use efficiency can be estimated using mechanistic models based on leaf biochemistry and micrometeorological parameters, but these models are complex and generally require many parameters that cannot be directly estimated by remote sensing [8]. Light use efficiency may be assumed to be constant under non-stress conditions, but it is affected by stresses, phenological stages, and the physical environment [10]. In some Asian countries, the value of ε has been estimated as 1.5 gC MJ^{-1} [31]. Here, we compare the output of mechanistic models of light use efficiency to the MODIS GPP product (MOD17) in the Denpasar area.

The main analysis in this research is to calculate GPP on different types of land use, but similar measures have been applied in analyzing the entire area of research. GPP maximum and minimum values are the maximum and minimum value of GPP in all research areas or a land use. Meanwhile the average value of GPP is obtained from division between the total value of GPP with the number of image pixels in all research areas or in each land use type. Analyses were carried out using ENVI 4.4 and ArcView GIS (version 3.2) software with the Spatial Analyst Extensions package.

3. Results and Discussion

3.1. Results

The two satellite datasets provide different estimates of annual GPP. With the ALOS/AVNIR-2 data, annual GPP varies from 0.13 gC m^{-2} yr^{-1} to 2,586.18 gC m^{-2} yr^{-1} with a mean of 836.23 gC m^{-2} yr^{-1}. With the Aster satellite, GPP shows a minimum of 0.14 gC m^{-2} yr^{-1}, a maximum of 2,595.26 gC m^{-2} yr^{-1}, and a mean of 776.83 gC m^{-2} yr^{-1}. Based on ALOS/AVNIR-2 data, total GPP

per year in Denpasar is 52,421.46 tC yr^{-1} and covers an area of 6,267.56 ha; the equivalent measures based on Aster satellite data are 59,355.49 tC yr^{-1} and 7,647.84 ha (Table 2). The GPP pixel value distribution from the ALOS/AVNIR-2 satellite data is dominated by low-GPP pixels (<250 gC m^{-2} yr^{-1}), which cover an area of 1,236.62 ha. The area covered decreases with increasing GPP; the highest GPP pixels (2,250–2,587 gC m^{-2} yr^{-1}) cover an area of 17.17 ha (Table 3). Similarly, the GPP pixel distribution from the Aster satellite data is also dominated by low-GPP pixels (<250 gC m^{-2} yr^{-1}), in this case covering an area of 1,694.56 ha, and area again decreases with increasing GPP. At the high end (GPP of 2,250–2,595 gC m^{-2} yr^{-1}), these pixels cover an area of 6.59 ha (Table 3). Maps of the GPP distribution from ALOS/AVNIR-2 and Aster are shown in Figure 2. In the Denpasar area, the maximum GPP measured by both ALOS/AVNIR-2 and Aster is smaller than the maximum GPP derived from the MOD17 (2,707.8 gC m^{-2} yr^{-1}).

Table 2. Annual GPP from the ALOS/AVNIR-2 and Aster satellites.

Satellite	GPP (gC m^{-2} yr^{-1})			Total GPP tC yr^{-1}
	Max	Mean	Min	
ALOS/AVNIR-2	2,586.18	836.23	0.13	52,421.46
Aster	2,595.26	776.83	0.14	59,355.49

Table 3. Total number of pixels and area covered for a range of GPP values from the ALOS/AVNIR-2 and Aster satellites.

GPP value (gC m^{-2} yr^{-1})	ALOS/AVNIR-2		Aster	
	Total pixels	Area (ha)	Total pixels	Area (ha)
< 250	123,662	1,236.62	75,314	1,694.56
250–500	101,694	1,016.94	59,523	1,339.27
500–750	88,378	883.78	49,242	1,107.94
750–1,000	76,929	769.29	42,346	952.78
1,000–1,250	70,423	704.23	36,175	813.94
1,250–1,500	61,249	612.49	30,336	682.56
1,500–1,750	52,544	525.44	24,785	557.66
1,750–2,000	34,440	344.40	14,900	335.25
2,000–2,250	15,720	157.20	6,990	157.27
> 2,250	1,717	17.17	293	6.59

Differences in land use can impact the measured annual GPP. The maximum GPP in the ALOS/AVNIR-2 data (2,586.18 gC m^{-2} yr^{-1}) was observed for a rice field, while the minimum (0.13 gC m^{-2} yr^{-1}) was observed for all types of land use. In the Aster data, the maximum GPP (2,595.26 gC m^{-2} yr^{-1}) was observed for forests (mangroves), while the minimum (0.14 gC m^{-2} yr^{-1}) was observed for all types of land use (Figure 3 and Table 4). Estimates of total annual GPP observed by ALOS/AVNIR-2 and Aster over different types of land use are shown in Table 4 and Figure 4.

Figure 2. Annual GPP distribution from two satellites: **(a)** ALOS/AVNIR-2 and **(b)** Aster.

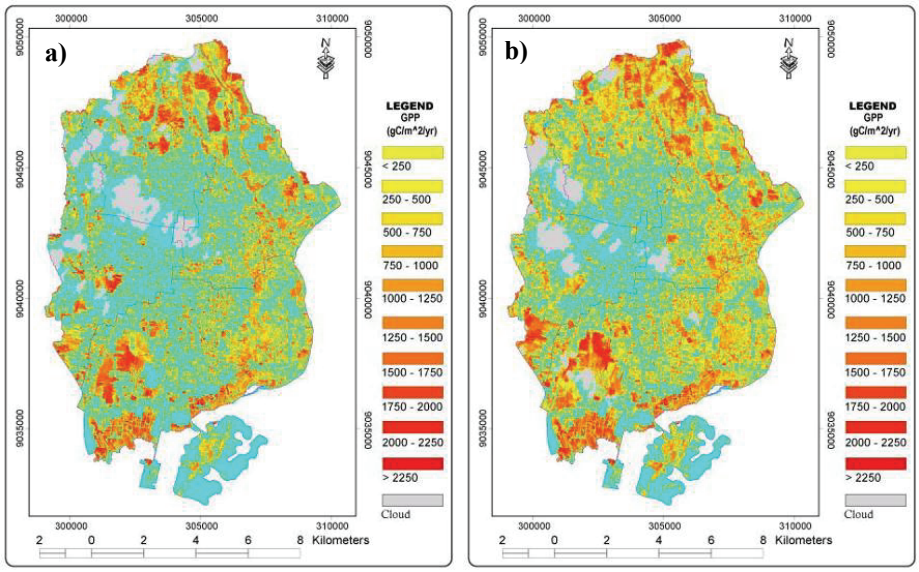

Figure 3. Annual GPP for different types of land use from ALOS/AVNIR-2 and Aster.

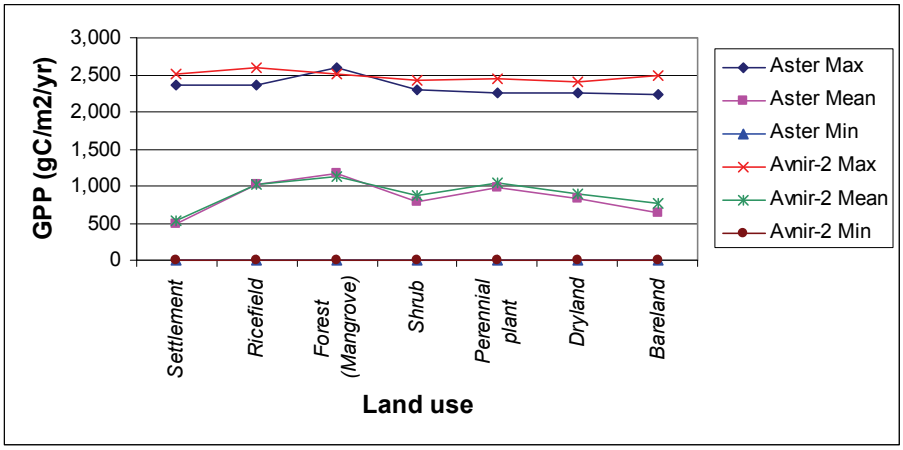

Table 4. Total annual GPP for different types of land use in the ALOS/AVNIR-2 and Aster data.

Land use	Area (Ha)	GPP (gC m^{-2} yr^{-1})						Total GPP (tC yr^{-1})	
		ALOS/AVNIR-2			Aster			ALOS/ AVNIR-2	Aster
		Max	Mean	Min	Max	Mean	Min		
Settlement	7,179.17	2,511.43	540.49	0.13	2,353.91	492.44	0.14	12,675.23	15,992.84
Rice field	2,616.34	2,586.18	1,030.08	0.13	2,371.86	1,020.65	0.14	20,254.15	22,571.65
Forest (Mangrove)	700.69	2,501.92	1,123.58	0.13	2,595.26	1,177.40	0.14	6,255.51	7,081.16
Shrub	81.10	2,427.54	882.11	0.13	2,305.14	794.37	0.14	469.55	460.96
Perennial plant	961.75	2,456.39	1,034.77	0.13	2,257.76	989.24	0.14	8,300.74	8,567.52
Dry land	263.26	2,414.05	893.46	0.13	2,261.80	830.61	0.14	1,888.87	1,930.72
Bare land	827.39	2,489.12	771.56	0.13	2,244.33	648.17	0.14	2,577.41	2,750.65

3.2. Discussion

In the Denpasar area of Bali, the GPP measured by the ALOS/AVNIR-2 and Aster satellites is smaller than that from the MODIS MOD17 product. This difference is primarily an artifact of the larger spectral range of MODIS. For MODIS, the spectral range is 0.05 micrometers for the red band

and 0.035 micrometers for the NIR band. Meanwhile, ALOS/AVNIR-2 has a spectral range of 0.08 micrometers in the red band and 0.13 micrometers in the NIR band, and Aster has a spectral range of 0.06 micrometers in the red band and 0.08 micrometers in the NIR band. The smaller spectral ranges of the ALOS/AVNIR-2 and Aster instruments increase the capability of these sensors to detect object on the surface. As spectral range decreases, the sensors lose the ability to map fine spectral features and to distinguish details [32]. The spectral range is directly related to both the material that is being identified by the sensor and the contrast between that material and the background materials [33].

Figure 4. Total annual GPP for different types of land use in the ALOS/AVNIR-2 and Aster data.

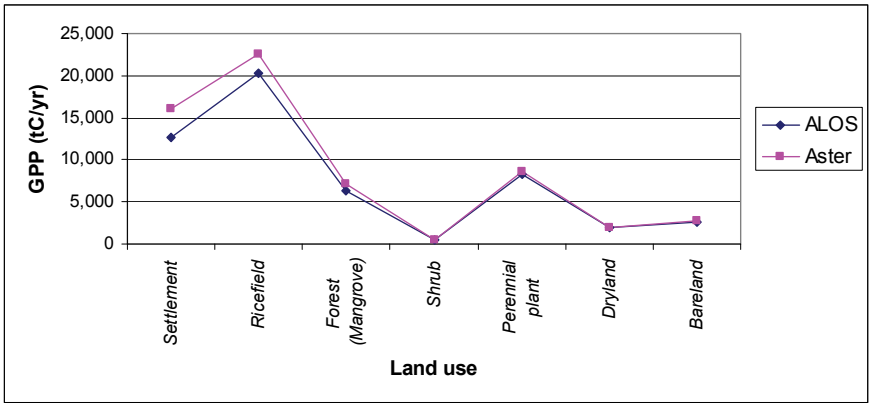

The top-of-atmosphere (TOA) reflectance in band 4 of AVNIR-2 appears to be lower than the TOA reflectance from exogenous sensor bands centered at 860 nm. This trait can be explained by the significant water vapor and dioxygen absorption that occurs in this band [27]. This difference in TOA reflectance may be responsible for the different estimate of annual GPP from ALOS/AVNIR-2.

Different values of GPP may also reflect differences in land use, which include differences in vegetation type, percent vegetation cover and dissemination. The measured vegetation index is related to the percent cover of vegetation in a given region [10,29]. Forests (mangroves) and rice fields are two types of land use that typically result in a higher mean GPP due to extensive and homogeneous vegetation cover. In contrast, areas dominated by settlements tend to have a higher maximum GPP but a lower mean GPP because the vegetation indices and GPP estimates of a given pixel are based on the average spectral value of that pixel. Denpasar is a unique city because it contains a "holy area" in the center of town that is characterized by extensive vegetation cover. The result is a high maximum GPP associated with settlement land use in Denpasar. Additional complication in the city comes from the fact that factories emitting CO_2 may be hidden beneath the same type of roof as found in residential areas. Additionally, canopy height fluctuations in the center of town are substantial and may cover many different types of land use. This creates a problem for subdividing urban areas into generalized classes of urban land use and activity based on the spectral values of each individual pixel [23].

The higher spatial resolution of ALOS/AVNIR-2 improves the detection of specific land use features, such as settlements, that lead to highly heterogeneous landscapes. As a result, ALOS/AVNIR-2 measured a higher GPP from settlement land use than Aster. In general, flux measurements are complicated in urban areas by surface heterogeneity, and NDVI becomes less important for scaling the CO_2 exchange [23].

The lower spatial resolution of Aster results in a higher total annual GPP from settlement land use than that measured by ALOS/AVNIR-2. The Aster satellite detects sparse vegetation around a settlement as a pixel with a low vegetation index rather than as a residential pixel. In other words, increased pixel size (or decreased spatial resolution) results in the loss of image detail [32]. Satellite data with high spatial resolution may be able to narrow the gap that currently exists between field measurements and remotely-sensed data from coarse-resolution satellites [34]. Improving spatial resolution is key to enhancing our ability to map detailed, scale-dependent variation. However, the image has high spatial resolution which has the disadvantage of having low spectral range, as also has been discussed previously by Lizarazo [35]. This condition causes the choice of image resolution is important to support the research goals.

4. Conclusion

Annual GPP measured by the ALOS/AVNIR-2 satellite is lower than that from Aster because ALOS/AVNIR-2 has a higher spatial resolution and smaller spectral range than Aster. Total GPP per year in Denpasar was 52,421.46 tC yr^{-1} as estimated by ALOS/AVNIR-2 and 59,355.49 tC yr^{-1} as estimated by Aster.

The medium spatial resolution of the remote sensing data is crucial for discriminating different land cover types in urban areas. Because of the heterogeneous land cover, the maximum value of GPP from ALOS/AVNIR-2 was smaller than that from Aster. Meanwhile, the annual mean GPP from ALOS/AVNIR-2 was higher than that from Aster because the higher spatial resolution of ALOS/AVNIR-2 results in improved detection of vegetation cover and conditions.

Estimates of GPP are affected by land use patterns. In particular, forests (mangroves) and rice fields are characterized by higher mean GPP. ALOS/AVNIR-2 estimates GPP as 1,123.58 gC m^{-2} yr^{-1} in forests (mangroves) and 1,030.08 gC m^{-2} yr^{-1} in rice fields; the totals from Aster are 1,177.40 gC m^{-2} yr^{-1} and 1,020.65 gC m^{-2} yr^{-1}, respectively. The lowest mean GPP was observed in land with settlements and was 540.49 gC m^{-2} yr^{-1} in the ALOS/AVNIR-2 data and 492.44 gC m^{-2} yr^{-1} in the Aster data.

The maximum GPP measured by ALOS/AVNIR-2 and Aster was smaller than the maximum from the MODIS GPP product (MOD17) in the Denpasar area, over a tropical peat swamp forest in central Kalimantan-Indonesia, and over a tropical forest in central Amazonia, Brazil.

Differences in spatial and spectral resolution affect the accuracy of object detection. For heterogeneous areas such as those containing settlements, satellites with high spatial resolution are necessary to detect detailed features. For homogeneous areas such as forests (mangroves) and rice fields, high spectral resolution is recommended.

Further research is needed to more accurately validate ALOS/AVNIR-2 and Aster GPP estimates. In particular, these satellites should be tested in areas with eddy flux towers so that satellite results can be directly compared to accurate *in situ* data.

Acknowledgments

Support for this work was provided by a JAXA, CReSOS and Indonesian department of national education (Diknas). Yasuhiro Sugimori and Abe Susanto kindly provided the image data and research costs.

References

1. Malhi, Y.; Nobre, A.D.; Grace, J.; Kruijt, B.; Pereira, M.G.P.; Culf, A.; Scott, S. Carbon dioxide transfer over a central Amazonian rain forest. *J. Geophys. Res.* **1998**, *103*, 593-612.
2. Hazarika, M.K.; Yasuoka, Y. Estimation of Terrestrial Carbon Fluxes by integrating Remote Sensing with Ecosystem Modeling. Ph. D. Dissertation, University of Tokyo, Tokyo, Japan, 2002.
3. Jenkins, J.P.; Richardson, A.D.; Braswell, B.H.; Ollinger, S.V.; Hollinger, D.Y.; Smith, M.L. Refining light-use efficiency calculations for a deciduous forest canopy using simultaneous tower-based carbon flux and radiometric measurements. *Agr. Forest Meteorol.* **2007**, *143*, 64-79.
4. Hunt, E.R.; Fahnestock, J.T.; Smith, W.K.; Kelly, R.D.; Welker, J.M.; Reiners, W.A. *Carbon Sequestration from Remotely Sensed NDVI and Net Ecosystem Exchange*; Muttiah, R.S., Ed.; Kluwer Academic Publishers: Dordrecht, The Netherlands, 2002.
5. Ibrahim, A.B. An Analysis of Spatial and Temporal Variation of Net Primary Productivity over Peninsular Malaysia Using Satellite Data. Ph. D. Thesis, University Technologi Malaysia, Johor, Malaysia, 2006.
6. Heinsch, F.A.; Reeves, M.; Votava, P.; Kang, S.; Milesi, C.; Zhao, M.; Glassy, J.; Jolly, W.M.; Loehman, R.; Bowker, C.F.; Kimball, J.S.; Nemani, R.R.; Running, S.W. *User's Guide GPP and NPP (MOD17A2/A3): Products NASA MODIS Land Algorithm*; Version 2, The University of Montana: Missoula, MT, USA, 2003.
7. Running, S.W.; Nemani, R.; Glassy, J.M.; Thornton, P.E. *MODIS Daily Photosynthesis (PSN) and Annual Net Primary Production (NPP) Product (MOD17)*; Algorithm Theoretical Basis Document (ATBD), Version 3.0, The University of Montana: Missoula, MT, USA, 1999.
8. Sims, D.A.; Luo, H.; Hastings, S.; Oechel, W.C.; Rahman, A.F.; Gamon, J.A. Parallel adjustments in vegetation greenness and ecosystem CO_2 exchange in response to drought in a southern California chaparral ecosystem. *Remote Sens. Environ.* **2006**, *103*, 289-303.
9. Monteith, J.L. Solar radiation and productivity in tropical ecosystems. *J. Appl. Ecol.* **1972**, *9*, 747-766.
10. Inoue, Y.; Peñuelas, J.; Miyata, A.; Mano, M. Normalized difference spectral indices for estimating photosynthetic hyperspectral and CO_2 flux measurements in rice. *Remote Sens. Environ.* **2008**, *112*, 156-172.
11. Turner, D.P.; Gowerb, S.T.; Cohenc, W.B.; Gregorya, M.; Maiersperger, T.K. Effects of spatial variability in light use efficiency on Satellite-Based NPP monitoring. *Remote Sens. Environ.* **2002**, *80*, 397-405.
12. Myneni, R.B.; Williams, D.L. On the relationship between FAPAR and NDVI. *Remote Sens. Environ.* **1994**, *49*, 200-211.
13. Hooda, R.S.; Dye, D.G. Estimating carbon-fixation in India based on remote sensing data. In *Proceedings of ACRS*, Colombo, Sri Lanka, November 1996.
14. La Puma, I.P.; Philippi, T.E.; Oberbauer, S.F. Development of a global evapotranspiration algorithm based on MODIS and global meteorology data. *Remote Sens. Environ.* **2007**, *109*, 225-236.

15. Hirano, T.; Harada, T.; Segah, H.; Limin, S.; June, T.; Hirata, R.; Osaki, M. CO_2 exchange of a tropical peat swamp forest in central Kalimantan. In *Proceedings of AsiaFlux Workshop 2005—International Workshop on Advanced Flux Network and Flux Evaluation*, Fujiyoshida, Japan, August 24–26, 2005.
16. Xiao, X.; Hollinger, D.; Aber, J.; Goltz, M.; Zhang, Q. Satellite-based modeling of gross primary production in an evergreen needle leaf forest. *Remote Sens. Environ.* **2004**, *89*, 519-534.
17. Xiao, X.; Zhang, Q.; Saleska, S.; Hutyra, L.; de Camargo, P.; Wofsy, S.; Frolking, S.; Boles, S.; Keller, M.; Moore, B. Satellite-based modeling of Gross Primary Production in a seasonally moist tropical evergreen forest. *Remote Sens. Environ.* **2005**, *94*, 105-122.
18. Saleska, S.R.; Miller, S.D.; Matross, D.M.; Goulden, M.L.; Wofsy, S.C.; da Rocha, H.R.; de Camargo, P.B.; Crill, P.; Daube, B.C.; de Freitas, H.C.; Hutyra, L.; Keller, M.; Kirchhoff, V.; Menton, M.; Munger, J.W.; Pyle, E.H.; Rice, A.H.; Silva, H. Carbon in Amazon forests: unexpected seasonal fluxes and disturbance-induced losses. *Science* **2003**, *302*, 1554-1557.
19. Nugroho, N.P. Estimating carbon sequestration in tropical rainforest using integrated remote sensing and ecosystem productivity modeling: A case study in Lebanan Concession Area, East Kalimantan, Indonesia. Ph.D. Thesis, International Institute for Geo-Information Science and Earth Observation (ITC), Enschede, The Netherlands, 2006.
20. Gitelson, A.A.; Viña, A.; Masek, J.G.; Verma, S.B.; Suyker, A.E. Synoptic monitoring of Gross Primary Productivity of maize using Landsat data. *IEEE Geosci. Remote Sens. Lett.* **2008**, *5*, 133-137.
21. Liang, S.; Zheng, T.; Wang, D.; Wang, K.; Liu, R.; Tsay, S.; Running, S.; Townshend, J. Mapping high-resolution incident photosynthetically active radiation over land from polar-orbiting and geo stationary satellite data. *Photogramm. Eng. Remote Sens.* **2007**, *73*, 1085-1089.
22. Yüksel, A.; Akay, A.E.; Gundogan, R. Using ASTER imagery in land use/cover classification of eastern Mediterranean landscapes according to CORINE land cover project. *Sensors* **2008**, *8*, 1237-1251.
23. Soegaard, H.; Møller-Jensen, L. Towards a spatial CO_2 budget of a metropolitan region based on textural image classification and flux measurements. *Remote Sens. Environ.* **2003**, *87*, 283-294.
24. Tang, J. The Analysis of Spatial-Temporal Dynamics of Urban Landscape Structure: A Comparison of Two Petroleum-Oriented Cities. Ph.D. Dissertation, Texas State University, San Marcos, TX, USA, 2007.
25. Li, F.; Kustas, W.P.; Anderson, M.C.; Prueger, J.H.; Scott, R.L. Effect of remote sensing spatial resolution on interpreting tower-based flux observations. *Remote Sens. Environ.* **2008**, *112*, 337-349.
26. Levin, N. Fundamentals of Remote Sensing. Available online: http://geography.huji.ac.il/personal/Noam%20Levin/1999-fundamentals-of-remote-sensing.pdf (accessed on 18 April 2010).
27. Saunier, S.; Rodriguez, Y.; Mambimba, A.; Goryl, P.; Grimont, P.; Bouvet, M.; Viallefont, F.; Santer, R.; Chander, G. *Consolidated Verification Report: AVNIR-2*; GAEL Consultant: Champs-sur-Marne, France, 2006.
28. Abrams, M; Hook, S. *ASTER User Handbook: Version 2*; Jet Propulsion Laboratory/California Institute of Technology: Pasadena, CA, USA, 2002.

29. Horning, N. *Global Land Vegetation: An Electronic Textbook*; NASA Goddard Space Flight Center Earth Sciences Directorate Scientific and Educational Endeavors (SEE): Greenbelt, MD, USA, 2004.
30. Waring, R.H.; Running, S.W. *Forest Ecosystems: Analysis at Multiple Scales*; Academic Press: New York, NY, USA, 1998.
31. Ochi, S.; Shibasaki, R. Estimation of NPP based agricultural production for Asian countries using remote sensing data and GIS. In *Proceedings of ACRS*, Tokyo, Japan, November 22–25, 1999.
32. Kruse, F.A. The effects of spatial resolution, spectral resolution, and SNR on geologic mapping using hyperspectral data, northern Grapevine Mountains, Nevada. In *Proceedings of the 9th JPL Airborne Earth Science Workshop*; Jet Propulsion Laboratory Publication, NASA: Greenbelt, MD, USA, 2000; pp. 261-269.
33. De Jong, S.M.; Van Der Meer, F.D. *Remote Sensing Image Analysis: Including the Spatial Domain*; Kluwer Academic Publishers: Dordrecht, The Netherlands, 2005.
34. Rocchini, D. Effects of spatial and spectral resolution in estimating ecosystem A-diversity by satellite imagery. *Remote Sens. Environ.* **2007**, *111*, 423-434.
35. Lizarazo, I. Urban land cover and land use classification using high spatial resolution images and spatial metrics. In *Proceedings of the 2nd Workshop of the EARSeL SIG on Land Use and Land Cover*, Bonn, Germany, September 2006; pp. 292-298.